Cerebral Cortex Advance Access published July 29, 2014

Cerebral Cortex
doi:10.1093/cercor/bhu161

Brain State Differentiation and Behavioral Inflexibility in Autism†

Lucina Q. Uddin[1,‡], Kaustubh Supekar[2,‡], Charles J. Lynch[2], Katherine M. Cheng[2], Paola Odriozola[2], Maria E. Barth[2], Jennifer Phillips[2], Carl Feinstein[2], Daniel A. Abrams[2] and Vinod Menon[2,3,4]

[1]Department of Psychology, University of Miami, Coral Gables, FL 33124, USA, [2]Department of Psychiatry and Behavioral Sciences, [3]Program in Neuroscience and [4]Department of Neurology and Neurological Sciences, Stanford University School of Medicine, Stanford, CA 94305, USA

†Portions of this data were presented at the Annual Meeting of the International Society for Autism Research 2013, San Sebastian, Spain.

‡Lucina Q. Uddin and Kaustubh Supekar contributed equally to this study.

Address correspondence to Lucina Q. Uddin, University of Miami, PO Box 248185-0751, Coral Gables, FL 33124, USA. Email: l.uddin@miami.edu

Autism spectrum disorders (ASDs) are characterized by social impairments alongside cognitive and behavioral inflexibility. While social deficits in ASDs have extensively been characterized, the neurobiological basis of inflexibility and its relation to core clinical symptoms of the disorder are unknown. We acquired functional neuroimaging data from 2 cohorts, each consisting of 17 children with ASDs and 17 age- and IQ-matched typically developing (TD) children, during stimulus-evoked brain states involving performance of social attention and numerical problem solving tasks, as well as during intrinsic, resting brain states. Effective connectivity between key nodes of the salience network, default mode network, and central executive network was used to obtain indices of functional organization across evoked and intrinsic brain states. In both cohorts examined, a machine learning algorithm was able to discriminate intrinsic (resting) and evoked (task) functional brain network configurations more accurately in TD children than in children with ASD. Brain state discriminability was related to severity of restricted and repetitive behaviors, indicating that weak modulation of brain states may contribute to behavioral inflexibility in ASD. These findings provide novel evidence for a potential link between neurophysiological inflexibility and core symptoms of this complex neurodevelopmental disorder.

Keywords: autism spectrum disorder, central executive network, default mode network, restricted and repetitive behaviors, salience network

Introduction

The ability to flexibly switch between different modes of thought is a critical feature of several aspects of human cognition. Cognitive flexibility is the readiness with which one can selectively switch between mental processes to appropriately respond to environmental stimuli (Scott 1962), and is thought to rely on distributed networks involving lateral prefrontal, posterior parietal, anterior cingulate, and anterior insular cortices (Dosenbach et al. 2007; Uddin et al. 2011; Cole et al. 2013). Cognitive "inflexibility" is a hallmark of autism spectrum disorders (ASDs), neurodevelopmental disorders characterized by social communication deficits, fixated interests, and repetitive behaviors. Measures of flexibility are predictive of symptom severity for repetitive behaviors in individuals with ASDs (Lopez et al. 2005; Van Eylen et al. 2011). At present, little is known regarding the neurobiological basis of this inflexibility.

Recent work has identified several core large-scale brain networks involved in coordinating flexible behaviors. Among these are (1) a fronto-parietal central executive network (CEN) comprised of the dorsolateral prefrontal cortex (DLPFC) and posterior parietal cortex (PPC), involved in the maintenance and manipulation of information and decision-making in the context of goal-directed behavior; (2) a default mode network (DMN) including the ventromedial prefrontal cortex (VMPFC) and posterior cingulate cortex (PCC), associated with self-related and social cognition; and (3) a salience network (SN) with key nodes in the right fronto-insular cortex (rFIC) and anterior cingulate cortex (ACC), involved in interoceptive, affective, attention, and control processes (Sridharan et al. 2008). An important function of the SN is to identify relevant internal and extrapersonal stimuli to guide flexible behavior (Seeley et al. 2007). It has recently been demonstrated that children with ASD exhibit intrinsic functional hyperconnectivity within the SN, CEN, and DMN (Uddin, Supekar, Lynch, et al. 2013) as well as other neural systems (Supekar, Uddin, et al. 2013). This within-network intrinsic hyperconnectivity in ASD may result in "network isolation" during task-evoked states, limiting dynamic interactions between brain networks that are necessary for flexible and adaptive cognition and behavior (Cole et al. 2013). The hypothesis that an intrinsically hyperconnected brain may result in aberrant dynamic processing during task-evoked states can be tested by examining causal interactions between brain regions.

Decades of studies using animal models suggest that hyperexcitability during critical periods for neural development can lead to highly undifferentiated brain states in later life (Rubenstein and Merzenich 2003). Yet, the role of brain state differentiation in human brain function is largely unknown. In addition, implications of these findings for typical and atypical human brain development have not been fully explored. In particular, no previous studies have explored the extent to which brain states are differentiated in ASD. It is unknown whether such mechanisms contribute to impairments in dynamic interactions between large-scale brain networks that might underlie cognitive and behavioral inflexibility in the disorder.

Both intrinsic and task-induced functional connectivity have widely been investigated in the human brain using fMRI (Biswal et al. 1995; Greicius et al. 2003; Schipul et al. 2012). Functional connectivity is a measure of temporal correlations between remote neurophysiological events, and effective connectivity is a measure of the influence one neural system exerts over another (Friston 1994; Seth 2010). An emerging literature suggests that, in young children with ASD, intrinsic functional hyperconnectivity can be observed across both cortical and subcortical systems (Di Martino et al. 2011; Keown et al. 2013; Supekar, Uddin, et al. 2013; Uddin, Supekar, Menon 2013).

Previous effective connectivity studies of ASDs have revealed reductions in causal connectivity between social brain regions in adolescents and adults with the disorder (Wicker et al. 2008; Deshpande et al. 2013; Hanson et al. 2013).

Here we used effective connectivity between nodes of the CEN, DMN, and SN in children with ASD and also in typically developing (TD) children as indices of network configuration across intrinsic and evoked brain states. We tested the hypothesis that intrinsic network hyperconnectivity recently documented in this population (Uddin, Supekar, Lynch, et al. 2013) is associated with reduced flexibility between intrinsic and evoked brain states. Additionally, we assessed whether these measures of brain state differentiation could be used to predict severity of behavioral impairment in children with ASD.

Materials and Methods

Participants

Participants were recruited in the San Francisco Bay Area through advertisements in school and local newspapers and fliers. Children with ASDs were also recruited from the Stanford Autism Clinic and the Lucille Packard Children's Hospital at the Stanford Medical Center. Data were collected from 2 cohorts, each consisting of children with ASD and TD children. Diagnosis of ASD was established using the Autism Diagnostic Interview (ADI-R; Lord et al. 1994) and the Autism Diagnostic Observation Schedule (ADOS, module 3; Lord et al. 2000) administered by assessors supervised by a research-reliable clinician (J.P.) (Table 1). Participants gave written informed assent, and parents or guardians gave written informed consent. The study was approved by the Stanford University Institutional Review Board.

MRI Data Acquisition

Task and resting-state fMRI data were acquired from the 2 cohorts of participants to allow for comparison of brain network dynamics between intrinsic and evoked states (Fig. 1*A*). The first experiment was an attention-demanding task with no social processing requirement. Children were asked to indicate whether visually presented single-digit arithmetic problems were correct or incorrect. The second experiment was an attention-demanding task using faces as stimuli, thus invoking social processing. This task used a visual oddball paradigm (Crottaz-Herbette et al. 2005) to elicit attention to social objects (e.g., faces). Tasks were chosen so as to require attention but not be overly difficult for children in this age range, to minimize group differences in behavioral performance.

Arithmetic Task and Rest

The first cohort of MRI data was collected from 17 children with ASD and 17 TD children matched on age and IQ. This cohort consisted of 16 male and 1 female participants in each group. Functional images were acquired on a 3-T GE Signa scanner (General Electric, Milwaukee, WI, USA) using a custom-built head coil (Glover and Lai 1998). Head movement was minimized during scanning by small cushions. A total of 29 axial slices (4.0 mm thickness and 0.5 mm skip) parallel to the AC–PC line and covering the whole brain were imaged using a T_2*-weighted gradient-echo spiral in-out pulse sequence (Glover and Law 2001) with the following parameters: time repetition (TR) = 2000 ms, echo time (TE) = 30 ms, flip angle = 80°, 1 interleave, for the duration of a 6 : 32 min task scan, and a 6-min resting-state scan. The field of view was 20 cm, and the matrix size was 64 × 64, providing an in-plane spatial resolution of 3.125 mm. To reduce blurring and signal loss arising from field inhomogeneities, an automated high-order shimming method based on spiral acquisitions was used before acquiring functional scans.

For the arithmetic verification task, 52 arithmetic problems were presented in a jittered event-related design along with "rest" or "null" trials in which participants passively viewed a cross on the screen. In the arithmetic trials, participants were presented with an equation involving 2 addends and a resultant and were asked to indicate via a button box whether the resultant was correct or incorrect. Half the addition trials consisted of problems with addends different from "1" (e.g., 3 + 4 = 7). One operand ranged from 2 to 9, the other from 2 to 5 (tie problems, such as "5 + 5 = 10," were excluded), and resultants were correct in 50% of the trials. Incorrect answers deviated by ±1 or ±2 from the correct sum. The remaining addition trials had the same format but one addend was "1" (e.g., 5 + 1 = 7). Stimuli were displayed for 5 s with an intertrial interval of 500 ms followed by a blank screen for 500 ms and an intertrial jitter that varied between 0 and 3500 ms with an average duration of 1814 ms. Details of the experimental design are described in previous studies (Supekar and Menon 2012).

For the 6-min resting-state scan, participants viewed the following instructions prior to beginning: "Relax. Please keep your eyes closed but do not go to sleep."

Social Attention Task and Rest

The second cohort of MRI data was collected from 17 children with ASD and 17 TD children matched on age and IQ. In this cohort, the ASD sample consisted of 16 male and 1 female participants, and the TD group consisted of 15 male and 2 female participants. The TD groups for the arithmetic and social attention task did not contain any overlapping participants. There was one participant with ASD who participated in both the arithmetic and social attention tasks separated by a 2-year gap between studies; the remaining 16 ASD participants in each study were nonoverlapping.

Functional images were acquired on a 3-T GE Signa scanner (General Electric) using a custom-built head coil. Head movement was minimized during scanning by small cushions. A total of 31 axial slices (4.0 mm thickness and 0.5 mm skip) parallel to the AC–PC line and covering the whole brain were imaged using a T_2*-weighted gradient-echo spiral in-out pulse sequence with the following parameters:

Table 1
Participant demographics

	Arithmetic task and rest data			Social attention task and rest data		
	ASD (n = 17)	TD (n = 17)	P-value	ASD (n = 17)	TD (n = 17)	P-value
Age	9.9 ± 0.4	9.8 ± 0.4	0.89	10.5 ± 0.3	9.6 ± 0.4	0.20
Gender	16M:1F	16M:1F		16M:1F	15M:2F	
Full-scale IQ	119.6 ± 3.9	119.6 ± 3.7	0.99	108.5 ± 3.8	116.4 ± 3.3[a]	0.13
Handedness	14R:3L	14R:3L		17R	17R	
ADOS Social	8.6 ± 0.4[b]			9.1 ± 0.5[b]		
ADOS Comm	3.4 ± 0.4[b]			3.7 ± 0.4[b]		
ADI-A	19.3 ± 1.4			19.6 ± 1.6[b]		
ADI-B	15.1 ± 1.4			15.8 ± 1.3[b]		
ADI-C	5.8 ± 0.8			6.8 ± 0.6[b]		

R, right; L, left; A, ambidextrous.
[a]Score missing for 1 participant.
[b]Score missing for 2 participants.

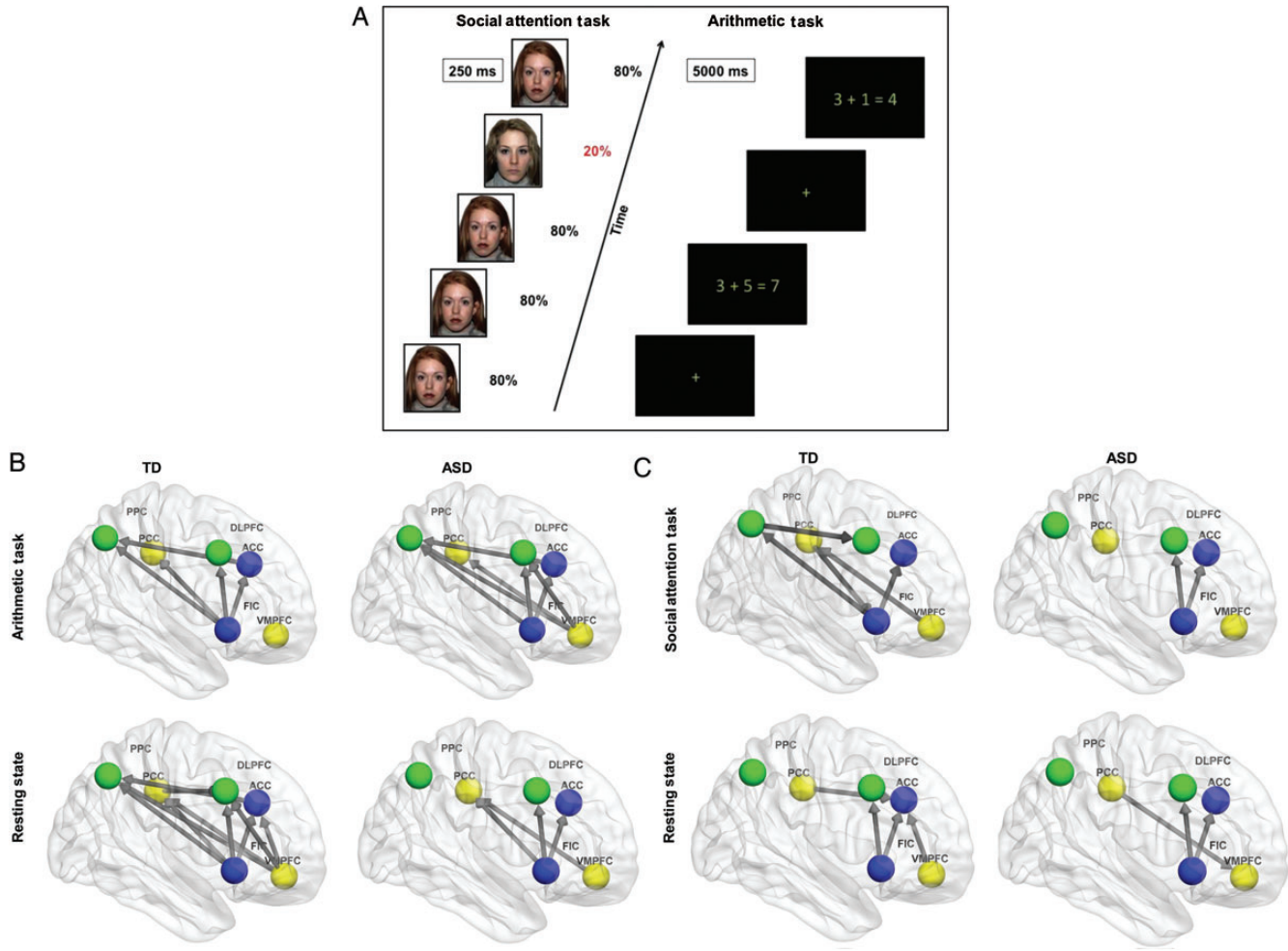

Figure 1. Effective connectivity between network nodes. (*A*) Social attention and arithmetic verification tasks were used to probe task-evoked brain states. (*B*) GCA of the 6 key nodes of the salience (blue), central executive (green), and default mode (yellow) networks in TD children and children with ASD during the arithmetic task, social attention task, and resting state. ROIs within the SN, right CEN, and DMN were based on a previous publication which identified these nodes using ICA of resting-state fMRI data (Uddin et al. 2011). Network nodes were based on 8-mm radius spheres created around coordinates from the previous study. ACC, anterior cingulate cortex; FIC, fronto-insular cortex; DLPFC, dorsolateral prefrontal cortex; PPC, posterior parietal cortex; VMPFC, ventromedial prefrontal cortex; PCC, posterior cingulate cortex. Figures were created using BrainNet Viewer (http://www.nitrc.org/projects/bnv/).

TR = 2000 ms, TE = 30 ms, flip angle = 80°, 1 interleave, for the duration of a 4-min task scan, and a 6-min resting-state scan.

A visual oddball attention task was used to assess brain responses to deviant stimuli. The oddball task is a simple paradigm that involves processing a sequence of events to detect a "target" deviant stimulus embedded in a stream of repetitive standard "nontarget" stimuli and measures orienting of attention and reflects an individual's ability to monitor the environment for change and decide on a course of action (Crottaz-Herbette and Menon 2006). For the current study, social visual stimuli (faces) were used. In an event-related design, each trial lasted 2 s, and each visual stimulus was presented for 250 ms. The intertrial interval was fixed at 2 s, and the interdeviant interval was 10 s with a standard deviation of 8 s. A total of 100 stimuli were presented. Two types of stimuli were presented: 80% of trials presented the "standard" stimulus (a female individual with a neutral expression) and 20% of trials presented the "deviant" stimulus (a different female individual with a neutral expression). The identity of the standard and deviant faces was counterbalanced across participants. Face stimuli were obtained from the NimStim Face Stimulus Set (http://www.macbrain.org/resources.htm; Tottenham et al. 2009). Participants were asked to press a button on a handheld response box with the right index finger in response to all standard stimuli, and to press another button with the right middle finger in response to the deviant stimuli.

As with the other cohort, for the 6-min resting-state scan, participants viewed the following instructions prior to beginning: "Relax. Please keep your eyes closed but do not go to sleep."

Structural MRI

For each subject, a high-resolution T_1-weighted spoiled grass gradient recalled inversion recovery 3D MRI sequence was acquired [inversion time (TI) = 300 ms, TR = 8.4 ms; TE = 1.8 ms; flip angle = 15°; 22 cm field of view; 132 slices in coronal plane; 256 × 192 matrix; 2 number of excitations, acquired resolution = 1.5 × 0.9 × 1.1 mm].

MRI Data Preprocessing

A linear shim correction was applied separately for each slice during reconstruction using a magnetic field map acquired automatically by the pulse sequence at the beginning of the scan. Functional MRI data were then analyzed using the SPM8 analysis software (http://www.fil.ion.ucl.ac.uk/spm). Images were realigned to correct for motion, corrected for errors in slice-timing, spatially transformed to standard stereotaxic space [based on the Montreal Neurologic Institute (MNI) coordinate system], resampled every 2 mm using sinc interpolation, and smoothed with a 6-mm full-width half-maximum Gaussian kernel to

Table 2
Neuroimaging data motion parameters

	Arithmetic task data			Social attention task data		
	ASD	TD	*P*-value	ASD	TD	*P*-value
Range *x*	1.21 ± 1.53	1.09 ± 1.33	0.80	0.79 ± 1.00	0.44 ± 0.41	0.20
Range *y*	1.89 ± 1.84	1.49 ± 1.63	0.51	1.28 ± 2.13	0.62 ± 0.69	0.24
Range *z*	3.37 ± 2.93	2.62 ± 2.76	0.45	1.65 ± 1.50	1.09 ± 0.87	0.19
Range pitch	3.22 ± 2.78	2.74 ± 2.50	0.60	2.29 ± 2.71	1.24 ± 1.62	0.18
Range roll	1.22 ± 0.86	1.47 ± 1.59	0.58	1.00 ± 1.36	0.57 ± 0.47	0.24
Range yaw	1.09 ± 0.93	1.10 ± 1.40	0.98	0.87 ± 1.12	0.50 ± 0.53	0.23
Maximum displacement	3.57 ± 2.88	3.28 ± 2.78	0.77	2.72 ± 2.85	1.73 ± 1.91	0.25
Maximum scan-to-scan displacement	3.60 ± 3.56	2.64 ± 2.80	0.39	1.76 ± 1.95	1.09 ± 0.94	0.22
Mean scan-to-scan displacement	0.34 ± 0.29	0.32 ± 0.30	0.83	0.22 ± 0.23	0.14 ± 0.12	0.18
	Rest data (same subjects as above)			Rest data (same subjects as above)		
	ASD	TD	*P*-value	ASD	TD	*P*-value
Range *x*	1.61 ± 2.17	1.07 ± 1.34	0.39	0.78 ± 1.00	0.84 ± 1.19	0.88
Range *y*	3.08 ± 4.51	1.90 ± 1.79	0.33	1.66 ± 2.51	0.86 ± 1.26	0.26
Range *z*	3.99 ± 4.18	3.06 ± 3.04	0.46	3.25 ± 5.09	1.53 ± 1.18	0.19
Range pitch	5.05 ± 5.80	4.07 ± 3.81	0.56	4.35 ± 6.87	2.70 ± 5.14	0.43
Range roll	1.70 ± 1.86	1.52 ± 1.77	0.78	1.06 ± 1.12	1.23 ± 2.20	0.78
Range yaw	1.49 ± 1.79	1.36 ± 1.58	0.83	0.86 ± 0.81	1.79 ± 5.24	0.48
Maximum displacement	6.04 ± 7.08	5.31 ± 5.16	0.73	5.13 ± 7.17	3.66 ± 6.15	0.53
Maximum scan-to-scan displacement	4.29 ± 5.45	3.15 ± 2.64	0.45	2.99 ± 5.46	1.74 ± 3.29	0.43
Mean scan-to-scan displacement	0.40 ± 0.45	0.25 ± 0.21	0.23	0.27 ± 0.33	0.19 ± 0.30	0.52

Table 3
Coordinates of ROIs

Network	Node	BA	Peak MNI coordinates
Salience network	R fronto-insular cortex	47	39 23 −4
	Anterior cingulate cortex	24	6 24 32
Central executive network	R dorsolateral prefrontal cortex	9	46 20 44
	R posterior parietal cortex	40	52 −52 50
Default mode network	Ventromedial prefrontal cortex	11	−2 38 −12
	Posterior cingulate cortex	23/30	−6 −44 34

decrease spatial noise prior to statistical analysis. Translational movement in millimeters (*x*, *y*, and *z*) and rotational motion in degrees (pitch, roll, and yaw) were calculated based on the SPM parameters for motion correction of the functional images in each subject. Motion parameters did not differ between children with ASD and TD children (Table 2).

Region of Interest Selection

We defined functional regions of interest (ROIs) in 6 key nodes of the SN, CEN, and DMN based on our recent previously published coordinates delineating these regions in an independent dataset (Uddin et al. 2011). In that study, independent component analysis (ICA) was used to identify the SN, DMN, and CEN in a combined group of children and adults. Functionally defined ROIs in key nodes of the SN, CEN, and DMN were based on the peaks of the ICA clusters. ROIs were selected from group ICA maps as follows: in the rFIC and ACC (on the SN ICA map); in the rDLPFC and rPPC (on the CEN ICA map); and in the VMPFC and PCC (on the DMN ICA map). After selecting voxels with the highest *Z* scores within each cluster on the functional map, the final ROIs were constructed by drawing spheres with centers as the seed-point and a radius of 8 mm (Table 3).

Effective Connectivity: Multivariate Granger Causal Analysis

Multivariate Granger causal analysis (GCA) was performed in accordance with the methods of Seth (2010). First, the mean time course from each ROI was extracted for all subjects. Each time series was then detrended and its temporal mean was removed. GCA was performed to test for causal influences between ROIs. The order of the vector autoregressive (VAR) model used for computation of the influence measure was selected using Bayesian information criterion (BIC). The model order as determined by BIC was 2 for all datasets analyzed. Differencing was not applied because the majority of data in each group was covariance stationary. We proceeded to construct group-wise causal connectivity graphs from these raw *F*-values as described next. We performed statistical inferencing on the causal connections using nonparametric analyses. Empirical null distributions of influence terms (*F*-values) and their differences were estimated nonparametrically by generating surrogate datasets under the null hypothesis that there are no causal interactions between the regions. To generate an instance of surrogate data, a Fourier transform was applied to each regional time series and the phase of the transformed signal was randomized. Inverse Fourier transform was then applied to generate one instance of surrogate data. This procedure ensures that the magnitude spectrum of the data is preserved while any causal interactions between various regions are eliminated. Test statistics were then computed by fitting the VAR model to the surrogate data. This procedure was repeated for several instances of surrogate data ($n = 500$) to obtain the null distribution of *F*-values and their differences. Those directed connections whose mean (across subjects in the group) was significantly different from the mean of the null (*F*-value) distribution were identified using statistical tests and a stringent threshold [$P < 0.01$, false discovery rate (FDR) corrected for multiple comparisons]. The stringent threshold was chosen to avoid potentially spurious causal links introduced by the low temporal resolution and hemodynamic blurring in the fMRI signal. In addition, a difference of influence (doi) term ($F_{x\to y} - F_{y\to x}$) was used to assess links that showed a dominant direction of influence; the difference term further limits potentially spurious links caused by hemodynamic blurring. Again, these dominant links were those wherein the mean of the difference of influence term significantly differed from the empirically constructed null distribution ($P < 0.01$, FDR corrected for multiple comparisons).

Classification Analysis: Discriminating Evoked Versus Intrinsic Connectivity Patterns

To assess the extent to which brain network patterns in evoked versus intrinsic states could be discriminated in both groups of participants, we used a multivariate statistical pattern recognition-based method. The effective connectivity patterns—strength of causal connectivity of 15 pairs of ROIs—were used as the input (features) to a multivariate pattern-based classifier. The classifier distinguishes evoked brain state from intrinsic brain state by making a classification decision based on the value of the nonlinear combination of these features. An advantage of using a multivariate classifier approach, as opposed to a traditional univariate *t*-test, is that a multivariate approach examines patterns of

causal connectivity across the entire networks, and is thus more sensitive. Therefore, our multivariate approach allows us to investigate the question of whether and to what extent causal connectivity patterns among the 6 ROIs during evoked brain states is different from those patterns during intrinsic brain states. Full details of this analysis are provided in Supplementary Material.

Relationship Between Brain State Discriminability and Symptom Severity: Correlation Analysis

To investigate relationships between brain state discriminability and symptom severity in children with ASD, we computed correlation coefficients between brain state discriminability and symptom severity based on diagnostic criteria (ADI-R Social, ADI-R Communication, ADI-R Repetitive Behavior, ADOS Social, and ADOS Communication Domain scores). Brain state discriminability was measured as the "distance" between the evoked and intrinsic brain states. The distance between each subject's evoked state and intrinsic state was computed by adding the distance of his/her evoked state from the hyperplane and the distance of his/her intrinsic state from the hyperplane. As the nonlinear SVM procedure attempts to find a hyperplane that represents the largest separation between the 2 classes (evoked state vs. intrinsic state), the distance from the hyperplane represents the discriminability of the observation. Using this measure of discriminability, we tested for significant correlations with scores on the 3 subscales of the ADI-R and the 2 subscales of the ADOS.

Relationship Between Brain State Discriminability and Symptom Severity: Prediction Analysis

The aforementioned correlation analysis provides information about the associative relationship between brain state discriminability and symptom severity in children with ASD. To assess the predictive ability of brain state discriminability, we used a novel machine learning approach—balanced cross-validation with linear regression (Supekar, Swigart, et al. 2013). Details of this procedure are described in Supplementary Material.

Relationship Between Brain State Discriminability and IQ

To further assess the significance of brain state discriminability for intellectual functioning, we conducted both correlation and prediction analyses using full-scale IQ for children with ASD and TD children.

Results

Behavioral Responses During Arithmetic and Social Attention Tasks

The children with ASD and TD groups did not differ on reaction time or accuracy on either the arithmetic task (ASD accuracy 0.89 ± 0.10, TD accuracy 0.83 ± 0.15, $P = 0.18$; ASD reaction time 2159.40 ± 479.70 ms, TD reaction time 2285.25 ± 314.53 ms, $P = 0.37$) or the social attention task (ASD accuracy 0.81 ± 0.18, TD accuracy 0.89 ± 0.13, $P = 0.20$; ASD reaction time 537.10 ± 171.19, TD reaction time 636.50 ± 167.80, $P = 0.12$, data missing from 3 ASD and 1 TD participant).

Task-Evoked Versus Intrinsic Effective Connectivity

We computed causal influences between the 6 network nodes for both the arithmetic task and the social attention task, as well as for the resting-state data collected from the same individuals. During both intrinsic and evoked brain states, both groups of children exhibited brain network dynamics consistent with previous observations that the rFIC acts as a "causal outflow hub" by influencing activity in other key network nodes (Sridharan et al. 2008; Uddin et al. 2011) (Fig. 1*B*,*C*).

Using these 2 datasets of task and resting-state fMRI data, we sought to examine whether children with ASD exhibit neurophysiological inflexibility. This was tested using a nonlinear SVM classification algorithm designed to assess the discriminability of effective connectivity measurements between intrinsic and evoked brain states within subjects in both experiments. This analysis revealed that task-related (evoked) and resting-state (intrinsic) effective connectivity measures were more discriminable in TD children than in children with ASD (Fig. 2*A*). In other words, brain states during task and rest from the same participant were more differentiated in TD children than in children with ASD.

Relationship Between Neural Inflexibility and Clinical Symptoms

We next sought to test whether this reduced differentiation between brain states in ASD was related to cognitive and behavioral inflexibility. We tested for relationships between symptom severity as measured by 2 subscales of the ADOS (Communication and Reciprocal Social Interaction) and 3 subscales of the ADI (Reciprocal Social Interaction, Communication, and Restricted, Repetitive, and Stereotyped Patterns of Behavior). We found that children with ASD who were most severely affected in the domain of restricted and repetitive behaviors showed the greatest degree of similarity between effective connectivity measures in task and rest during the arithmetic task ($r = -0.51$, $P = 0.02$), with a similar trend in the social attention task ($r = -0.47$, $P = 0.07$) (Fig. 2*B*,*C*). We further examined the predictive ability of these connectivity measures using a machine learning approach. Results from this analysis showed that the degree of similarity between effective connectivity measures in task and rest during the arithmetic task [$r(\text{pred,actual}) = 0.47$, $P = 0.03$] and the social attention task [$r(\text{pred,actual}) = 0.35$, $P = 0.06$] predicted symptom severity in the domain of restricted and repetitive behaviors. Neither the correlative nor predictive relationships between brain state discriminability and symptom severity were observed for any other subscale of the ADI or the ADOS for either task. Thus, the brain–behavior relationships were observed only with restricted and repetitive behaviors, and not with measures of social communication. Relationships between brain state discriminability and IQ were also explored. Children with ASD and TD children showed no significant correlations or predictions using full-scale IQ.

Discussion

In addition to well-documented social communication impairments, a key characteristic of ASD is the presence of restricted and repetitive behaviors, cognitive inflexibility, and a "need for sameness" (Turner 1999). Despite the prevalence and severity of cognitive and behavioral inflexibility in ASD, there is no unifying hypotheses or model to describe the link between these core symptoms and brain dynamics. We show that characterizing brain network dynamics in ASD during evoked and intrinsic states can provide novel insights into the etiology and complex phenotype of the disorder.

In the current work, we sought to uncover neural signatures of behavioral inflexibility by examining dynamic interactions among 3 core neurocognitive networks implicated in developmental psychopathology—the default mode, salience, and

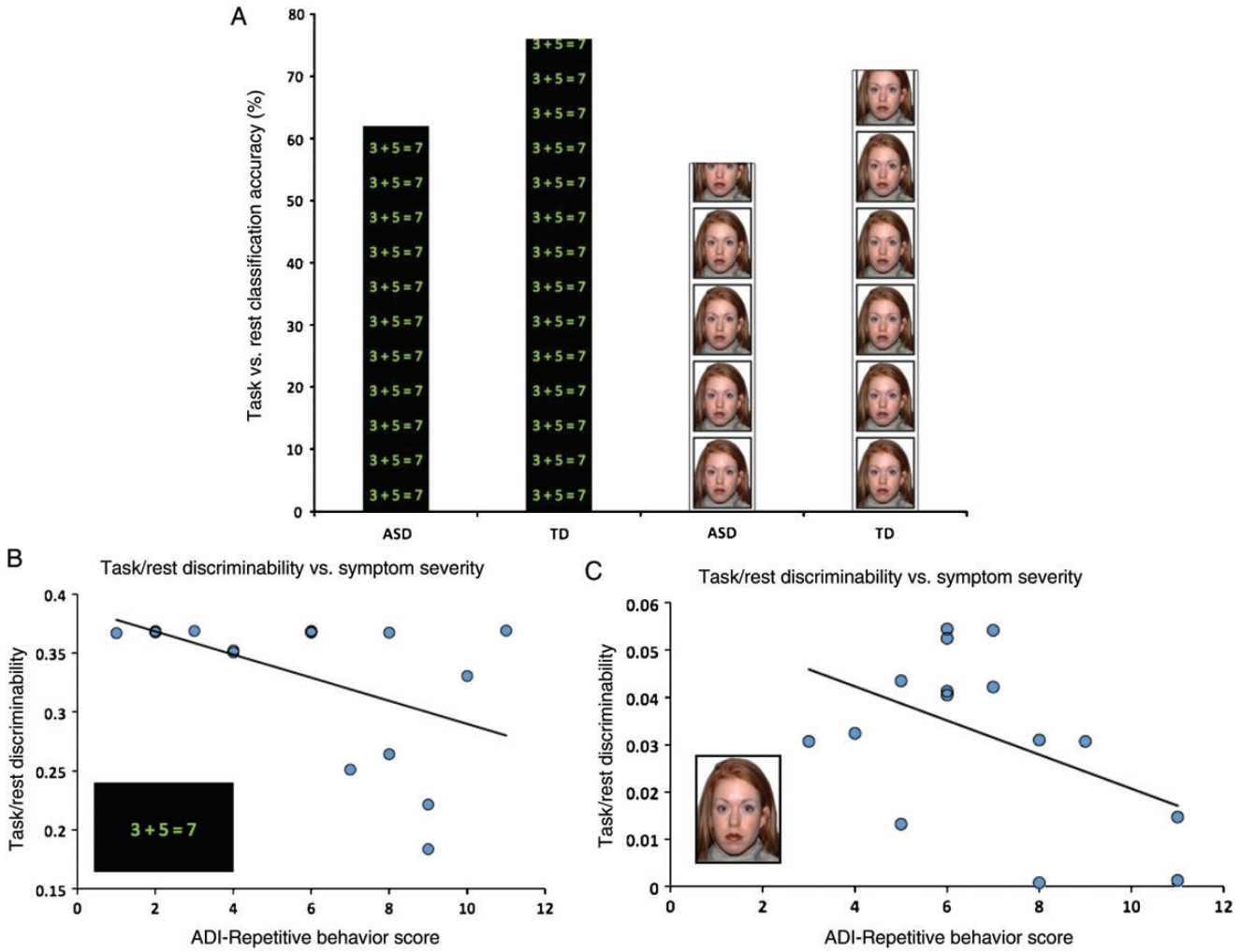

Figure 2. Brain state discriminability and relation to clinical symptoms. (*A*) Effective connectivity measures computed for task and resting-state data were subjected to classification analyses to determine, within each individual, the extent to which the 2 brain states could be discriminated. For both the arithmetic and social attention task, evoked and intrinsic brain states were discriminated with a high degree of accuracy in TD children, in contrast with results observed in children with ASD. (*B*) Children with ASD who were most severely affected on restricted and repetitive behaviors showed the greatest degree of similarity between causal connectivity measures in the arithmetic task and rest ($n = 17$; $r = -0.51$, $P = 0.02$), (*C*) and to some degree in the social attention task and rest ($n = 15$; $r = -0.47$, $P = 0.07$). As can be seen in *B* and *C*, task/rest discriminability scores were overall much higher for the arithmetic task than for the social attention task.

CENs (Menon 2011). We have recently shown that the causal influence of the rFIC "hub" on nodes of the salience and CENs is significantly greater in adults compared with TD children, and have suggested that functional maturation of rFIC pathways is critical to the development of brain networks capable of supporting complex, flexible cognitive processes in adulthood (Uddin et al. 2011). Here, we leveraged the insights gained from recent examinations of these core brain networks to explore the extent to which the brain in ASD shows reduced differentiation, as previously hypothesized based on animal models (Rubenstein and Merzenich 2003). Our results suggest that atypical brain network dynamics may contribute to cognitive and behavioral inflexibility in autism.

Using patterns of effective connectivity between 6 key nodes of 3 neurocognitive networks (DMN, SN, and CEN), we found evidence for reduced discriminability between evoked and intrinsic brain states in children with ASD. Specifically, children with ASD do not exhibit as drastic changes in connectivity patterns between task-evoked processing and resting states as do TD children. This finding is in line with the hypothesis that autism may be characterized by "undifferentiated brain states" (Rubenstein and Merzenich 2003) as animal models suggest.

In 2 cohorts of children, we demonstrate that evoked and intrinsic connectivity patterns are more differentiated in TD children than in children with ASD. This neurophysiological inflexibility in ASD reflects weaker task-dependent modulation and aberrant functional connectivity in the disorder (Kana et al. 2011; Just et al. 2012). We recently demonstrated intrinsic functional hyperconnectivity across multiple large-scale brain networks including the DMN, SN, and CEN in children with ASD, and suggested that this hyperconnectivity may hinder network interactions necessary for flexible behavior (Uddin, Supekar, Lynch, et al. 2013). Here we show that across 2 tasks with different instructions, cognitive demands, and stimuli, similar patterns of neurophysiological inflexibility can be observed in ASD. The current data provide the first empirical evidence integrating noisy neural processing and aberrant functional connectivity models of ASD.

While the idea that altered patterns of functional connectivity underlie the diverse symptoms observed in autism has dominated the field (Kana et al. 2011; Just et al. 2012), previous studies have focused on characterizing task-related connectivity (Muller et al. 2011) or more recently, intrinsic connectivity in isolation (Uddin, Supekar, Menon 2013). However, understanding the neural basis of behavioral inflexibility requires concurrent examination of both intrinsic and evoked brain states. Recent work by You et al. (2013) has demonstrated atypical modulation of long-range functional connectivity patterns in children with ASD as they transition from intrinsic resting states to attention-demanding task-evoked brain states. The work by You and colleagues is consistent with previous studies providing evidence for noisy processing and unreliable evoked responses (Dinstein et al. 2012) and altered patterns of connectivity across cognitive states in ASD (Barttfeld et al. 2012). Previous studies used static measures of functional connectivity, and did not characterize effective connectivity between brain regions for flexible cognitive control in ASD. Here, we show that dynamic interactions between 3 core neurocognitive networks are differentially modulated by task performance in TD children compared with children with ASD.

Behaviorally, autism manifests as a need for sameness, cognitive rigidity, and an inability to flexibly adapt behavior in novel situations. These behaviors are linked to brain function in our sample of children with ASD. We found a significant positive correlation between task/rest discrimination and restricted and repetitive behavior symptoms as measured by the ADI. The ADI Restricted and Repetitive Behavior subscale quantifies individual's preoccupation or circumscribed patterns of interests, compulsive adherence to nonfunctional routines or rituals, stereotyped and repetitive motor mannerisms, and preoccupation with parts of objects or nonfunctional elements of material (Lord et al. 1994). As measures of cognitive flexibility are predictive of symptom severity for repetitive behaviors in autism (Lopez et al. 2005), this ADI subscale serves as a proxy for flexibility deficits in this population. Reduced differentiation between evoked and intrinsic brain states was more prominent in children who were most severely impaired in the restricted and repetitive behavior domain. The differentiation between evoked and intrinsic brain states was also predictive of severity of impairment in the restricted and repetitive behavior domain in children with ASD. Severity of social and communication deficits was not related to the brain state measures computed, nor was IQ, suggesting that there may be a specific link with behavioral inflexibility symptoms of ASD. While the behavioral relationships tested in the current study are not exhaustive, the current findings suggest that weaker modulation between task-evoked and intrinsic brain states may underlie the behavioral manifestations of restricted and repetitive behaviors and cognitive inflexibility that characterize this complex disorder. Future work with larger samples and more comprehensive behavioral and cognitive test batteries including the Repetitive Behavior Scale (Lam and Aman 2007) will be necessary to test the specificity of the brain–behavior links reported here.

It should be noted that, in addition to the cortical systems emphasized in the current study, atypical development of subcortical structures such as the basal ganglia has also been shown to contribute to restricted and repetitive behaviors in ASD (Langen et al. 2009). Incorporating network models that include cortical and subcortical components is thus an important direction for future research. In the current study, we present a novel approach for investigating brain state discriminability, revealing ASD-related atypicalities. The specificity of these findings to ASD will need to be assessed in future studies of other neurodevelopmental disorders affecting brain connectivity and behavioral flexibility.

Supplementary Material

Supplementary material can be found at: http://www.cercor.oxfordjournals.org/.

Funding

This work was supported by a NIMH Career Development Award (K01MH092288) and a Slifka/Ritvo Innovation in Autism Research Award from the International Society for Autism Research to L.Q.U., as well as grants from the National Institutes of Health (HD047520, HD059205, and MH084164 to V.M.), the National Science Foundation (BCS/DRL 0449927), and the Singer Foundation to V.M.

Notes

The authors thank Dirk Neumann for providing critical feedback, Amirah Khouzam, Christina Young, Caitlin Tenison, and Sangeetha Santhanam for assistance with data collection, and Srikanth Ryali for contributing data analytic tools. *Conflict of Interest*: None declared.

References

Barttfeld P, Wicker B, Cukier S, Navarta S, Lew S, Leiguarda R, Sigman M. 2012. State-dependent changes of connectivity patterns and functional brain network topology in autism spectrum disorder. Neuropsychologia. 50:3653–3662.

Biswal B, Yetkin FZ, Haughton VM, Hyde JS. 1995. Functional connectivity in the motor cortex of resting human brain using echo-planar MRI. Magn Reson Med. 34:537–541.

Cole MW, Reynolds JR, Power JD, Repovs G, Anticevic A, Braver TS. 2013. Multi-task connectivity reveals flexible hubs for adaptive task control. Nat Neurosci. 16:1348–1355.

Crottaz-Herbette S, Lau KM, Glover GH, Menon V. 2005. Hippocampal involvement in detection of deviant auditory and visual stimuli. Hippocampus. 15:132–139.

Crottaz-Herbette S, Menon V. 2006. Where and when the anterior cingulate cortex modulates attentional response: combined fMRI and ERP evidence. J Cogn Neurosci. 18:766–780.

Deshpande G, Libero LE, Sreenivasan KR, Deshpande HD, Kana RK. 2013. Identification of neural connectivity signatures of autism using machine learning. Front Hum Neurosci. 7:670.

Di Martino A, Kelly C, Grzadzinski R, Zuo XN, Mennes M, Mairena MA, Lord C, Castellanos FX, Milham MP. 2011. Aberrant striatal functional connectivity in children with autism. Biol Psychiatry. 69:847–856.

Dinstein I, Heeger DJ, Lorenzi L, Minshew NJ, Malach R, Behrmann M. 2012. Unreliable evoked responses in autism. Neuron. 75:981–991.

Dosenbach NU, Fair DA, Miezin FM, Cohen AL, Wenger KK, Dosenbach RA, Fox MD, Snyder AZ, Vincent JL, Raichle ME et al. 2007. Distinct brain networks for adaptive and stable task control in humans. Proc Natl Acad Sci USA. 104:11073–11078.

Friston K. 1994. Functional and effective connectivity in neuroimaging: a synthesis. Hum Brain Mapp. 2:56–78.

Glover GH, Lai S. 1998. Self-navigated spiral fMRI: interleaved versus single-shot. Magn Reson Med. 39:361–368.

Glover GH, Law CS. 2001. Spiral-in/out BOLD fMRI for increased SNR and reduced susceptibility artifacts. Magn Reson Med. 46:515–522.

Greicius MD, Krasnow B, Reiss AL, Menon V. 2003. Functional connectivity in the resting brain: a network analysis of the default mode hypothesis. Proc Natl Acad Sci USA. 100:253–258.
Hanson C, Hanson SJ, Ramsey J, Glymour C. 2013. Atypical effective connectivity of social brain networks in individuals with autism. Brain Connectivity. 3:578–589.
Just MA, Keller TA, Malave VL, Kana RK, Varma S. 2012. Autism as a neural systems disorder: a theory of frontal-posterior underconnectivity. Neurosci Biobehav Rev. 36:1292–1313.
Kana RK, Libero LE, Moore MS. 2011. Disrupted cortical connectivity theory as an explanatory model for autism spectrum disorders. Phys Life Rev. 8:410–437.
Keown CL, Shih P, Nair A, Peterson N, Mulvey ME, Muller RA. 2013. Local functional overconnectivity in posterior brain regions is associated with symptom severity in autism spectrum disorders. Cell Rep. 5:567–572.
Lam KS, Aman MG. 2007. The Repetitive Behavior Scale-Revised: independent validation in individuals with autism spectrum disorders. J Autism Dev Disord. 37:855–866.
Langen M, Schnack HG, Nederveen H, Bos D, Lahuis BE, de Jonge MV, van Engeland H, Durston S. 2009. Changes in the developmental trajectories of striatum in autism. Biol Psychiatry. 66:327–333.
Lopez BR, Lincoln AJ, Ozonoff S, Lai Z. 2005. Examining the relationship between executive functions and restricted, repetitive symptoms of autistic disorder. J Autism Dev Disord. 35:445–460.
Lord C, Risi S, Lambrecht L, Cook EH Jr, Leventhal BL, DiLavore PC, Pickles A, Rutter M. 2000. The autism diagnostic observation schedule-generic: a standard measure of social and communication deficits associated with the spectrum of autism. J Autism Dev Disord. 30:205–223.
Lord C, Rutter M, Le Couteur A. 1994. Autism Diagnostic Interview-Revised: a revised version of a diagnostic interview for caregivers of individuals with possible pervasive developmental disorders. J Autism Dev Disord. 24:659–685.
Menon V. 2011. Large-scale brain networks and psychopathology: a unifying triple network model. Trends Cogn Sci. 15:483–506.
Muller RA, Shih P, Keehn B, Deyoe JR, Leyden KM, Shukla DK. 2011. Underconnected, but how? A survey of functional connectivity MRI studies in autism spectrum disorders. Cereb Cortex. 21:2233–2243.
Rubenstein JL, Merzenich MM. 2003. Model of autism: increased ratio of excitation/inhibition in key neural systems. Genes Brain Behav. 2:255–267.
Schipul SE, Williams DL, Keller TA, Minshew NJ, Just MA. 2012. Distinctive neural processes during learning in autism. Cereb Cortex. 22:937–950.
Scott WA. 1962. Cognitive complexity and cognitive flexibility. Sociometry. 25:405–414.
Seeley WW, Menon V, Schatzberg AF, Keller J, Glover GH, Kenna H, Reiss AL, Greicius MD. 2007. Dissociable intrinsic connectivity networks for salience processing and executive control. J Neurosci. 27:2349–2356.
Seth AK. 2010. A MATLAB toolbox for Granger causal connectivity analysis. J Neurosci Methods. 186:262–273.
Sridharan D, Levitin DJ, Menon V. 2008. A critical role for the right fronto-insular cortex in switching between central-executive and default-mode networks. Proc Natl Acad Sci USA. 105:12569–12574.
Supekar K, Menon V. 2012. Developmental maturation of dynamic causal control signals in higher-order cognition: a neurocognitive network model. PLoS Comput Biol. 8:e1002374.
Supekar K, Swigart AG, Tenison C, Jolles DD, Rosenberg-Lee M, Fuchs L, Menon V. 2013. Neural predictors of individual differences in response to math tutoring in primary-grade school children. Proc Natl Acad Sci USA. 110:8230–8235.
Supekar K, Uddin LQ, Khouzam A, Phillips J, Gaillard WD, Kenworthy LE, Yerys BE, Vaidya CJ, Menon V. 2013. Brain hyperconnectivity in children with autism and its links to social deficits. Cell Rep. 5:738–747.
Tottenham N, Tanaka JW, Leon AC, McCarry T, Nurse M, Hare TA, Marcus DJ, Westerlund A, Casey BJ, Nelson C. 2009. The NimStim set of facial expressions: judgments from untrained research participants. Psychiatry Res. 168:242–249.
Turner M. 1999. Annotation: repetitive behaviour in autism: a review of psychological research. J Child Psychol Psychiatry. 40:839–849.
Uddin LQ, Supekar K, Lynch CJ, Khouzam A, Phillips J, Feinstein C, Ryali S, Menon V. 2013. Salience network-based classification and prediction of symptom severity in children with autism. JAMA Psychiatry. 70:869–879.
Uddin LQ, Supekar K, Menon V. 2013. Reconceptualizing functional brain connectivity in autism from a developmental perspective. Front Hum Neurosci. 7:458.
Uddin LQ, Supekar KS, Ryali S, Menon V. 2011. Dynamic reconfiguration of structural and functional connectivity across core neurocognitive brain networks with development. J Neurosci. 31:18578–18589.
Van Eylen L, Boets B, Steyaert J, Evers K, Wagemans J, Noens I. 2011. Cognitive flexibility in autism spectrum disorder: explaining the inconsistencies? Res Autism Spectr Disord. 5:1390–1401.
Wicker B, Fonlupt P, Hubert B, Tardif C, Gepner B, Deruelle C. 2008. Abnormal cerebral effective connectivity during explicit emotional processing in adults with autism spectrum disorder. Soc Cogn Affect Neurosci. 3:135–143.
You X, Norr M, Murphy E, Kuschner ES, Bal E, Gaillard WD, Kenworthy L, Vaidya CJ. 2013. Atypical modulation of distant functional connectivity by cognitive state in children with Autism Spectrum Disorders. Front Hum Neurosci. 7:482.